


Hydrodynamic ex-vivo analysis of valve sparing techniques: assessment and comparison

Sofia Di Leonardo^{1*}, Danila Vella^{1*}, Carmelo Savio Grillo², Carla Martorana², Salvatore Torre^{2,3},
Vincenzo Argano^{2,3}, Gaetano Burriesci^{1,4}


¹Bioengineering Group, Ri.MED Foundation, Palermo, Italy

²School of Medicine and Surgery, University of Palermo, Italy

³Cardiac Surgery Unit, Policlinico Paolo Giaccone, University of Palermo, Italy

⁴UCL Mechanical Engineering, University College London, UK

*Contributed equally

Corresponding author (Gaetano Burriesci, UCL Mechanical Engineering, Torrington place,
London, WC1E7JE, UK (+44)02076793922, g.burriesci@ucl.ac.uk)

Meeting presentation

This work was selected for presentation at the 36th EACTS Annual Meeting.

Word count: 4982

21 **Visual Abstract**

- 22 • Key question: what is the impact of the valve-sparing procedure and graft configuration on the
23 predicted aortic valve performance?
- 24 • Key findings: dynamics and performance of the aortic root strongly depend on the graft
25 configuration.
- 26 • Take-home message: grafts replicating Valsalva sinuses can restore more physiological valve
27 dynamics and performances.

28

29 **Abstract**

30

31 **Objectives:** Valve-sparing procedures are surgical techniques allowing to restore adequate function of the
32 native aortic valve by replacing the dysfunctional ascending aorta with a prosthetic conduit. A number of
33 techniques are currently used, such as Yacoub's remodelling and David's reimplantation, based on a regular
34 straight conduit. More recently, the De Paulis proposed the use of bulging conduits to reconstruct the shape
35 of the Valsalva sinuses. This work investigates the impact of the valve-sparing technique on the aortic valve
36 function.

37 **Methods:** The performance of three porcine aortic roots (Medtronic Freestyle™) was assessed in a
38 cardiovascular pulse duplicator before and after performing three alternative valve-sparing procedures:
39 David's reimplantation, Yacoub's remodelling and De Paulis' reimplantation.

40 **Results:** The porcine aortic roots, representative of the healthy native configuration, were characterised by the
41 highest efficiency, with a mean energetic dissipation under normal operating conditions of 26 mJ. David's
42 and Yacoub's techniques resulted in significantly lower performance (with mean energetic loss of about 70 mJ
43 for both cases). The De Paulis' procedure exhibited intermediate behaviour, with superior systolic
44 performance and valve dynamics similar to the native case, and a mean energetic loss of 38 mJ.

45 **Conclusions:** The dynamics and performance after valve-sparing strongly depend on the adopted technique,
46 with the use of conduits replicating the presence of Valsalva sinuses restoring more physiological conditions.

47

48 **Keywords:** Valve-sparing implants; Aortic root prosthesis; Hydrodynamic performance; Ex-vivo analysis;
49 Valsalva sinuses

50

51 **1. Introduction**

52 Despite its apparently simple anatomical morphology, the aortic root has the function to establish and
53 maintain a haemocompatible intermittent laminar flow, proper coronary perfusion and optimum left ventricular
54 function at the different operating conditions [1]. This involves a synergistic interplay between its different
55 constituent elements at both, microscopic and macroscopic level. Dysfunctional pathologies such as
56 aneurysms of the ascending aorta can alter these delicate mechanisms, resulting into major complications. In
57 fact, abnormal dilation of the arterial vessel in proximity of the aortic valve can cause dislocation of the
58 commissures, with consequent lack of coaptation of the valve leaflets, independently of their structural

59 integrity. This may result in a clinical condition of aortic insufficiency, associated with reduced left ventricular
60 function and ejection fraction, potentially leading to acute pulmonary edema [2].

61 Aneurysmal pathology of the aortic root is normally treated through traditional surgical therapies, aimed at
62 repairing the aortic root and resolve aortic insufficiency.

63 When the insufficiency has functional nature, and the native valve leaflets have maintained their integrity, their
64 physiological function and anatomy can be restored by adopting common valve-sparing procedures [3], such
65 as the David's 'reimplantation' technique [4], and the Yacoub's 'remodelling' technique [5]. In both
66 approaches, the three sinuses of Valsalva are excised from the native root and replaced with a tubular straight
67 graft. In particular, in David's procedure, the proximal edge of the graft is sutured at the annulus, whilst in the
68 case of Yacoub's procedure it is cut into a crown shape and sutured just above the leaflets attachment. Over
69 the years, several reports have suggested that although Yacoub's remodelling procedure is physiologically
70 superior to David's reimplantation procedure, with a more natural motion of the aortic annulus, it may be
71 associated with higher risk of annulo-aortic ectasia and recurring insufficiency [6], [7]. David's technique,
72 instead, provides a better stabilisation of the aortic annulus, but the total removal of the Valsalva sinuses has
73 been associated with suboptimal hemodynamics [8].

74 More recently, De Paulis *et al.* proposed a readaptation of both techniques, replacing the tubular graft with a
75 Gelweave Valsalva™ (Vascutek, UK) graft, that incorporates a bulging segment that can replicate the presence
76 of the Valsalva sinuses [9]. In this case, the commissures of the native valve are stitched to the graft at the
77 level of the suture between the bulging segment and the tubular portion of the prosthesis, acting as a sino-
78 tubular junction (STJ). Although the use of this graft is described for both, reimplantation and remodelling
79 procedures, De Paulis *et al.* indicate it as particularly suitable to perfection the David's technique, as it could
80 allow a more physiological leaflets dynamics, whilst stabilising the annulus diameter.

81 Over the years different studies investigated the performances of tubular and Valsalva conduits and the efficacy
82 of reproducing Valsalva sinuses, finding discordant results [10], [11]. These results clearly expose that the
83 optimal conduit for valve-sparing still needs to be identified [12], and the role of the Valsalva sinuses on the
84 hemodynamics is far from being agreed upon.

85 This work presents an analysis and comparison of the hydrodynamic performance of the most common
86 aortic root repair procedures, namely the David's reimplantation, Yacoub's remodelling and De Paulis'
87 reimplantation, with the healthy native reference. The aim of the work is to assess the ability of each technique
88 to restore healthy operating conditions by means of systematic in-vitro testing, and verify if the attempt to
89 restore the morphology of the Valsalva sinuses can provide a clinical advantage.

90

91 **2. Materials and Methods**

92

93 **2.1. Prosthesis implants**

94 The Medtronic Freestyle™ bioprosthetic aortic root was selected to represent healthy native operating
95 conditions. This device consists of a porcine aortic root, cross-linked in dilute glutaraldehyde solution while

96 applying 40 mmHg of internal pressure on the root (after ligating the coronary arteries at their inlet), to
97 counteract shrinkage and maintain the natural commissural configuration. Leaflets undergo chemical fixation
98 at zero differential pressure, thus minimising changes in their flexibility and function. The valve inflow edge
99 is covered with PET fabric, that extends over the ventricular muscle band present below the right coronary
100 ostium, in order to strengthen this region (see **Error! Reference source not found.**) [13]. Despite some
101 difference of proportion between the leaflets and the position in the coronary ostia, this prosthesis is recognised
102 to closely emulate the healthy human aortic root in terms of anatomy and function [14]. Three prosthetic roots
103 of size 25 mm (corresponding to the annulus diameter) were selected to represent healthy native conditions,
104 and tested in the pulse duplicator to assess their hydrodynamic performance. They were then used to perform
105 three surgical valve-sparing techniques, and retested for each configuration. The surgical procedures were
106 performed by the same experienced surgical team, in the following order: David's, Yacoub's and De Paulis'.

107 Before the implants, each graft was prepared by washing out the collagen coating and dipping the clean
108 fabric in a silicone suspension (1-2577 Low VOC) to make it impermeable to the saline solution used as test
109 fluid in the in-vitro assessments. For the David's and Yacoub's techniques, a straight tubular graft made of
110 surgical PET knitted fabric (Intergard) of 28 mm was used to achieve an increased sinuses diameter. David's
111 reimplantation technique was performed by excising the Valsalva sinuses from the native root, just leaving
112 few millimetres of aortic wall at the valve outflow. The proximal end of the tubular graft was sutured at the
113 annulus, immediately below the aortic valve. The outflow edge was sutured to the graft wall (see **Error!**
114 **Reference source not found.**). The Yacoub's configuration was directly derived from the David's, by
115 removing the suture points at the aortic annulus and trimming a three-pointed crown below the sutured line at
116 the outflow edge. Subsequently, the graft was removed and the valve sutured into a Gelweave Valsalva™
117 conduit of 26 mm diameter, performing the reimplantation procedure as described by De Paulis *et al.* [9]
118 (details about the surgical technique are reported in the Supplementary data, S1).

119 All implants were fixed to a specifically designed 3D printed resin support, in order to minimise distortion
120 during handling and allow easy and consistent positioning into the Pulse Duplicator for the hydrodynamic
121 assessment (see **Error! Reference source not found.**).

122

123 2.2. In-vitro testing

124 The hydrodynamic performance assessment of each implant was conducted in-vitro on a hydro-mechanical
125 pulse duplicator (ViVibro Superpump, SP3891, Canada). The system is composed of a servo controlled
126 volumetric pump that allows the fluid circulation in three cardiac chambers separated by exchangeable heart
127 valves. The fluid sections are equipped with an electromagnetic flowmeter (Carolina Medical, USA) and
128 pressure transducers (Utah Medical, USA) placed in all cardiac chambers.

129 All roots were tested in the aortic position, following the order of the procedures (healthy native, David,
130 Yacoub and De Paulis). A St Jude 29 mm bileaflet mechanical valve was used in the mitral position. In
131 compliance with the in-vitro test procedure of the ISO5840 standard [15], tests were carried out at six cardiac
132 outputs (CO: 2, 3, 4, 5, 6 and 7 l/min), at a heart rate 70 bpm, with systolic duration 35% and mean aortic

133 pressure equal to 100 mmHg. Buffered saline solution at room temperature was used as test fluid. For each
134 test, results were acquired over ten consecutive cycles, reporting their mean and standard deviation (SD).

135 The systolic performance was quantified on the basis of the mean systolic transvalvular pressure difference
136 measured during the positive differential pressure period (ΔP), and EOA was calculated based on the Gorlin's
137 formula [16], as in equation (1):

$$EOA = \frac{Q_{vRMS}}{51.6 \sqrt{\frac{\Delta P}{\rho}}} \quad (1)$$

138 where Q_{vRMS} is the root mean square forward flow (mm/s), ρ is the density of the test fluid (g/ml), and ΔP is
139 expressed in mmHg.

140 The diastolic performance was associated with the closing regurgitant volume (CRV), calculated as the
141 integral of the flow curve during the closing valve period.

142 The global performance during the whole cardiac cycle was quantified on the basis of the left ventricular
143 energy loss (E_{loss}) [17], [18], calculated as the sum of the forward flow energy loss (E_{lossF} , measured during
144 the ejection phase) and the closing energy loss (E_{lossC} , measured during the closing phase), determined in mJ
145 from equation (2) [19]:

$$E_{loss} = 0.1333 \int_{t_i}^{t_f} \Delta p \cdot q \cdot dt \quad (2)$$

146 where t_i and t_f are the initial and final time instants of the phase where the energetic loss is quantified, Δp
147 is the instantaneous transvalvular pressure, and q is the instantaneous flow rate (mm/s).

148 High frame rate (HFR) videos were recorded from the valve outflow at a CO of 5 l/min, to observe the
149 valve dynamics in the different implants. These videos were binarised and analysed with a code specifically
150 written in Matlab (MathWorks, USA) to quantify the instantaneous and mean projected orifice area (POA)
151 [20].

152 Videos of the sagittal view were also analysed in Matlab to determine the variation of diameter occurring
153 at the STJ during the cardiac cycle and compute the compliance as described in the ISO5840 [15].

154

155 **2.3. Statistical analysis**

156 The performance parameters at CO of 5 l/min were analysed using an Anova test for repeated measures. Where
157 a statistical difference was found, the Tukey honestly significant difference test was used to perform the post-
158 hoc pairwise comparison. A p-value $P < 0.05$ was considered statistically significant. The size effect was
159 estimated to evaluate the magnitude of the group differences, computing omega square (Ω^2). A $\Omega^2 > 0.14$ was
160 considered as large size effect [21].

161

162 3. Results

163 3.1. Hydrodynamic performances

164 The performance parameters determined for each test are summarised in the diagrams in **Error! Reference**
165 **source not found.**, where each column corresponds to a prosthesis.

166 For each valve, the ΔP indicates the best performance for the healthy native valve, with a mean value at 5
167 l/min of 4.49 mmHg, followed by the De Paulis' (mean of 6.45 mmHg). The David's and Yacoub's techniques
168 resulted in similarly higher ΔP (mean of 9.07 and 8.76 mmHg, respectively), with the remodelling approach
169 resulting slightly superior for valve 1 and slightly worse for the other two (see **Error! Reference source not**
170 **found.a-c**). Globally, ΔP is statistically different among the groups ($P = 0.002$) with a large size effect ($\Omega^2 =$
171 0.36), however the pairwise comparison does not result in any significant differences. The EOA reflects similar
172 trends (**Error! Reference source not found. d-f**), resulting maximum for the three healthy native valves (with
173 a mean value for all CO of 3.50 cm^2), followed by the De Paulis' (mean of 3.04 cm^2). The David's and
174 Yacoub's (mean of 2.53 and 2.44 cm^2 , respectively) mostly overlap at lower values. These differences are
175 statistically significant, with $P < 0.001$ and a large size effect of $\Omega^2 = 0.63$. Moreover, the post-hoc comparison
176 identifies significant differences in healthy native vs David ($P = 0.015$) and healthy native vs Yacoub ($P =$
177 0.015) (in Table S2.1 of section 'Supplementary data S2', the details of Tukey HSD post-hoc comparison are
178 reported). The energetic contribution of the systolic phase (E_{lossF} in **Error! Reference source not found.**),
179 is substantially lower for the healthy native configuration, followed by the De Paulis', which presents values
180 more than 50% higher. For the David's and Yacoub's implants, these losses are about twice as for the De
181 Paulis'.

182 All valves were fully competent in all configurations, with minimum leakage. The CRV has a variable
183 trend (see **Error! Reference source not found. g-I**), with the David's implants characterised by more stable
184 values among the tested COs (however difference is not statistically significant). In general, at high COs
185 (equal or greater than 5 l/min) the healthy native valve and Yacoub's (the two cases where the valve annulus
186 is not constrained into the graft) appear to undergo larger CRV. The E_{lossC} results minimum for the De Paulis',
187 intermediate for the David's and Yacoub's, and highest for the Freestyle (see **Error! Reference source not**
188 **found.**). However, this loss has lower contribution compared to the systolic, and does not alter considerably
189 the energetic efficiency of the different configurations. In fact, over the whole cycle, the E_{loss} (see **Error!**
190 **Reference source not found. l-n**) confirms that the healthy native configuration is more efficient for all COs
191 (with a mean value at 5 l/min of 26.24 mJ). The David's and Yacoub's are characterised by substantially
192 higher E_{loss} (70.89 and 73.26 mJ, respectively), while the De Paulis' is much closer to the healthy native
193 (37.84 mJ). The significance of the observed differences is confirmed by a $P < 0.001$ and a large size effect
194 $\Omega^2 = 0.76$. The post-hoc comparison results in significant differences between all groups, but David vs. Yacoub
195 (see Table S2.1 of section 'Supplementary data S2').

196 Table 1 summarises the performance parameters obtained for all valves and configurations, at a standard
197 CO of 5 l/min (in Table S3.2 of the Supplementary data S3, performance parameters at all COs are reported).

198 3.2. HFR video analysis

199 The mean POA values indicate that the estimated EOA closely correspond to the geometric leaflets opening
200 (see **Error! Reference source not found.**). Again, the healthy native valve exhibits the widest orifice area,
201 with the De Paulis' implant is associated with a decrease of POA of at least 10%, and the David's and Yacoub's
202 implants with a reduction of about 30% (healthy native > 3.16 cm²; David = 2.20 cm², Yacoub = 2.25 cm²,
203 De Paulis = 2.81 cm²).

204 Regarding the measured compliance, the healthy native displayed the highest value, equal to 11.5%. The
205 David's implant had the smallest elasticity of 3.3%, whilst Yacoub's technique was effective in restoring some
206 elasticity, increasing the compliance to 6.7%. The presence of corrugated sinuses in the De Paulis' provided
207 an increased compliance of 7.9%; the largest after the native root.

209 4. Discussion

210 All valves well exceeded the EOA requirements specified in the ISO5840 standard, which for the size of
211 25 mm requires values ≥ 1.45 cm² at 5 l/min (all implants had a mean EOA > 2.54 cm²). Still, despite the same
212 implantation size, the three aortic roots exhibited some differences in the hydrodynamic behaviour. In
213 particular, valve 2 appeared to be characterised by softer leaflets than the others, allowing wider opening and
214 lower ΔP for all procedures. On the contrary, valve 3 resulted slightly more stenotic, with opening areas 15-
215 20% smaller and ΔP about 60% higher than the other prostheses.

216 Nevertheless, the changes in performance parameters determined by each procedure were consistent for all
217 three valves, confirming statistically significant trends.

218 As expected, the healthy native valves were characterised by the best efficiency. This appears to be driven
219 by the superior physiological leaflets dynamics, with the leaflets expanding deep into the Valsalva sinuses to
220 maximise the EOA, so as to minimise the ΔP and the associated E_{loss} . Analysis of the images in **Error!**
221 **Reference source not found.** shows that large portions of the leaflets expand further than the window of
222 observation (this, represented as a red dashed line, has a diameter of 24 mm), with exception of the leaflet
223 positioned at the bottom. This, for all valves, corresponds to the leaflet adjacent to the ventricular muscle
224 band, stiffened by the presence of the PET fabric covering (represented in **Error! Reference source not**
225 **found.**), which reduces the leaflet ability to expand into the right coronary sinus. The opening mechanism
226 appears to be facilitated by the large compliance of the native aortic root, which undergoes relevant radial
227 expansion during systole, increasing the EOA even further.

228 The use of a tubular graft in the David's and Yacoub's techniques, with consequent alteration of the sinus
229 chambers, introduces a physical arrest to the valve leaflets which limits the achievable EOA. This levels the
230 performance for the two approaches. The Yacoub's approach appears to double the compliance of the implant
231 (3.3-6.7%), thanks to the three-pointed crown at the leaflet attachment. In particular, compared to the native
232 root, the two techniques were characterised by a reduction of EOA and a major increase in ΔP (at a CO of
233 5 l/min, EOA was 25-38% lower and ΔP was 75-140% larger for the three valves). This is well reflected in

234 the measurement of the POA, which shows a mean reduction of about 30% compared to the healthy native
235 valve, easy to be visually appreciated in **Error! Reference source not found.**

236 The attempt to replicate the presence of the Valsalva sinuses in the De Paulis' procedure appears effective
237 in restoring a more physiological dynamics, with the leaflets allowed to expand into the more pronounced
238 bulging section of the graft. De Paulis' results in better systolic performance than the other two valve-sparing
239 techniques, with an EOA reduced of just 10-15% compared to the healthy native configuration at a CO of 5
240 l/min (see Table 1). Again, this is well aligned with the results from the POA measurement.

241 Performing all sets of implants following the same sequence may introduce an order effect in the results.
242 However, this option was preferred as it allows to minimise the valve manipulations due to the removal and
243 re-suturing of the different grafts. In fact, adopting the selected sequence, only one suturing is requested for
244 the David's and Yacoub's, and a second one for the De Paulis. Still, the configuration experiencing the largest
245 number of manipulations, which is always the De Paulis, exhibits the best performance in all the three sparing
246 procedures, proving that any bias introduced during manipulation is not substantial, nor sufficient to alter the
247 order of the most favourable conditions.

248 In general, the wider leaflets expansion characterising the healthy native root is accompanied by some
249 larger closing backflow than the other solutions, except for valve 2, where the leaflets expand substantially
250 also after all valve-sparing procedures. This is a crucial result, as it challenges the most commonly accepted
251 theory in the literature, which regards the presence of the Valsalva sinuses as functional to generate and host
252 the vortices facilitating the valve closing [22], [23]. Instead, the presented tests appear to confirm the
253 mechanism recently proposed by Tango *et al.* [24] on the basis of a computational study of the idealised aortic
254 root. This identifies the main role of the sinuses in supporting the systolic phase by providing a chamber where
255 the leaflets can fully expand to reduce their interference with the ejected blood flow. In fact, as clearly
256 displayed in **Error! Reference source not found.**, the E_{loss} typically associated with the systolic forward flow
257 is far more relevant than that produced by the closing regurgitant flow. Hence, optimising the opening phase
258 can offer massive advantages, that make tolerable some collateral, but minor, loss in the closing phase.

259 From a clinical perspective, the presented study indicates that the De Paulis' technique can result in better
260 performance than the approaches based on tubular grafts, due to its ability to better reproduce the anatomy of
261 the Valsalva sinuses and their contribution to a larger valve opening [10]. However, it needs to be observed
262 that this result is inconsistent with a recent study reported by Paulsen *et al.* [11], [12]. This describes similar
263 in-vitro tests, but concludes that valve-sparing techniques based on the De Paulis' approach provide inferior
264 performance than reimplantation procedures performed with straight tubular conduits. This appears to be
265 associated with some major leakage measured with bulging grafts, possibly due to the implantation of the
266 commissures below the sino-tubular graft suture. This, in fact, may cause excessive radial dislocation of the
267 valve commissures, causing some degree of infra-valvular diastolic backflow (as in operating conditions
268 typical of aneurysmal roots). Hence, although our findings indicate the De Paulis' technique as potentially
269 superior, this outcome is necessarily procedural dependent, with the positioning of the commissures playing
270 an essential role. In fact, as described, excessively low positioning of the valve may result in the insurgence

271 of central leakage. On the contrary, excessively high positioning would obliterate the function of the sinuses,
272 making them unable to provide adequate room to host the expanding leaflets. The presented study also reveals
273 the potential role that in-vitro tests may play in perfecting surgical techniques and supporting clinical training.

274 **4.1. Study limitations**

275 The interpretation of the described findings shall take into consideration few approximations and limitations
276 in the performed tests. The anatomy and mechanical properties of the glutaraldehyde treated juvenile pig aortic
277 root are expected to have some difference from the corresponding patient's component. Also, the saline
278 solution used in the presented tests, and preferred to blood equivalents to prevent tissue changes that may affect
279 the tissue properties between tests, has different physical properties from human blood.

280 Moreover, the reduction of David's and Yacoub's techniques performances compared to the healthy native
281 configuration may be related with the inability of the procedure to generate anatomically ideal sinuses, and to
282 the lower compliance of the fabric graft. The similarity between the David's and Yacoub's techniques may be
283 justified by the utilization of a bio-root with a stiffened annulus, trigons and muscular ridge, as opposed to the
284 human valve. This may reduce the compliance achievable in human with the Yacoub's procedure.

285 Despite the adopted sample size provides statistically significant results about the differences between the
286 alternative procedures (with large size effect), larger sizes might, in future tests, increase the confidence in the
287 presented findings.

288

289

290 **5. Conclusions**

291 This work analyses and compares the hydrodynamic alterations introduced by the most common aortic root
292 repair procedures: David's reimplantation, Yacoub's remodelling and De Paulis' reimplantation.

293 The prostheses representative of the healthy aortic root expectedly resulted the most efficient, with
294 maximum EOA, and minimum ΔP and E_{loss} . This shows that, despite providing generally good performance,
295 current valve sparing techniques are still suboptimal and far from matching the physiological leaflets dynamics.
296 The significantly superior efficiency observed with the De Paulis' reimplantation technique confirms that
297 replicating the anatomical features of the aortic root may contribute to enhance the efficacy of the treatment.
298 Still, engineering improvement is needed to design conduits that better model the optimum compliance of the
299 native vessel.

300

301

302 **Data availability statement**

303 All relevant data are within the manuscript and its Supplementary data files, further data underlying
304 this article will be shared on reasonable request to the corresponding author.

305

306 **Conflict of interest: none declared.**

307

308 *Table 1 Implant performance parameter at 5 l/min of CO (distance from the healthy native result).*

| Valve | Configuration | ΔP [mmHg] | EOA [cm ²] | CRV [ml] | $E_{lossF} + E_{lossC}$ [mJ] |
|-------|---------------|-------------------|--------------------------|---------------|------------------------------|
| 1 | Native | 3.74 SD:0.12 | 3.81 SD:0.07 | -2.26 SD:0.15 | 21.60 SD:1.07 |
| | David | 9.53 SD:0.25 | 2.36 SD:0.02 (-38%) | -1.69 SD:0.07 | 75.05 SD:1.50 |
| | Yacoub | 9.07 SD:0.14 | 2.52 SD:0.03 (-34%) | -1.83 SD:0.17 | 68.47 SD:1.63 |
| | De Paulis | 5.36 SD:0.19 | 3.41 SD:0.06 (-10%) | -1.72 SD:0.09 | 36.81 SD:1.94 |
| 2 | Native | 3.66 SD:0.10 | 3.96 SD:0.05 | -2.38 SD:0.14 | 25.03 SD:1.08 |
| | David | 6.73 SD:0.07 | 2.91 SD:0.01 (-27%) | -2.52 SD:0.25 | 58.70 SD:1.54 |
| | Yacoub | 6.32 SD:0.09 | 2.84 SD:0.02 (-28%) | -2.60 SD:0.17 | 57.65 SD:1.66 |
| | De Paulis | 4.84 SD:0.23 | 3.38 SD:0.08 (-15%) | -2.00 SD:0.07 | 34.87 SD:1.06 |
| 3 | Native | 6.06 SD:0.13 | 3.24 SD:0.04 | -2.39 SD:0.14 | 32.10 SD:1.49 |
| | David | 10.97 SD:0.20 | 2.36 SD:0.02 (-25%) | -2.03 SD:0.10 | 78.93 SD:1.62 |
| | Yacoub | 10.88 SD:0.29 | 2.27 SD:0.03 (-28%) | -1.87 SD:0.11 | 93.67 SD:1.74 |
| | De Paulis | 9.15 SD:0.13 | 2.76 SD:0.02 (-12%) | -2.29 SD:0.14 | 41.86 SD:1.26 |

309

310 **Figure legend**

311 Figure 1. FreeStyle prosthesis. Sagittal, inflow and outflow views.

312 Figure 2. David implant steps: a) equipment, b) Native valve cutting, c) valve preparation, d) graft suturing,
313 final implant e) transversal and f) sagittal views.

314 Figure 3. healthy native prosthesis and valve-sparing implants, David, Yacoub and De Paulis, set into resin
315 support.

316 Figure 4. Implant performance parameter diagram of: a-c) ΔP ; d-f) EOA ; g-i) CRV ; l-n) $E_{lossF} + E_{lossC}$.
317 Each diagram reports mean performances value in 10 cycles. The standard deviation is reported as error bars.

318 Figure 5. Mean E_{lossC} and E_{lossF} for each kind of implant.

319 Figure 6. HFR images corresponding to the POA maximum value.

320 Central Image: Stacked bar graph representing the estimated forward (bottom) and closing (top) energy
321 losses for the healthy native prosthesis and for the De Paulis', David's and Yacoub's valve-sparing implants.
322

323
324 **References**

325 [1] H.-H. Sievers *et al.*, "The everyday used nomenclature of the aortic root components: the tower of
326 Babel?," *Eur. J. Cardio-Thoracic Surg.*, vol. 41, no. 3, pp. 478–482, Mar. 2012.

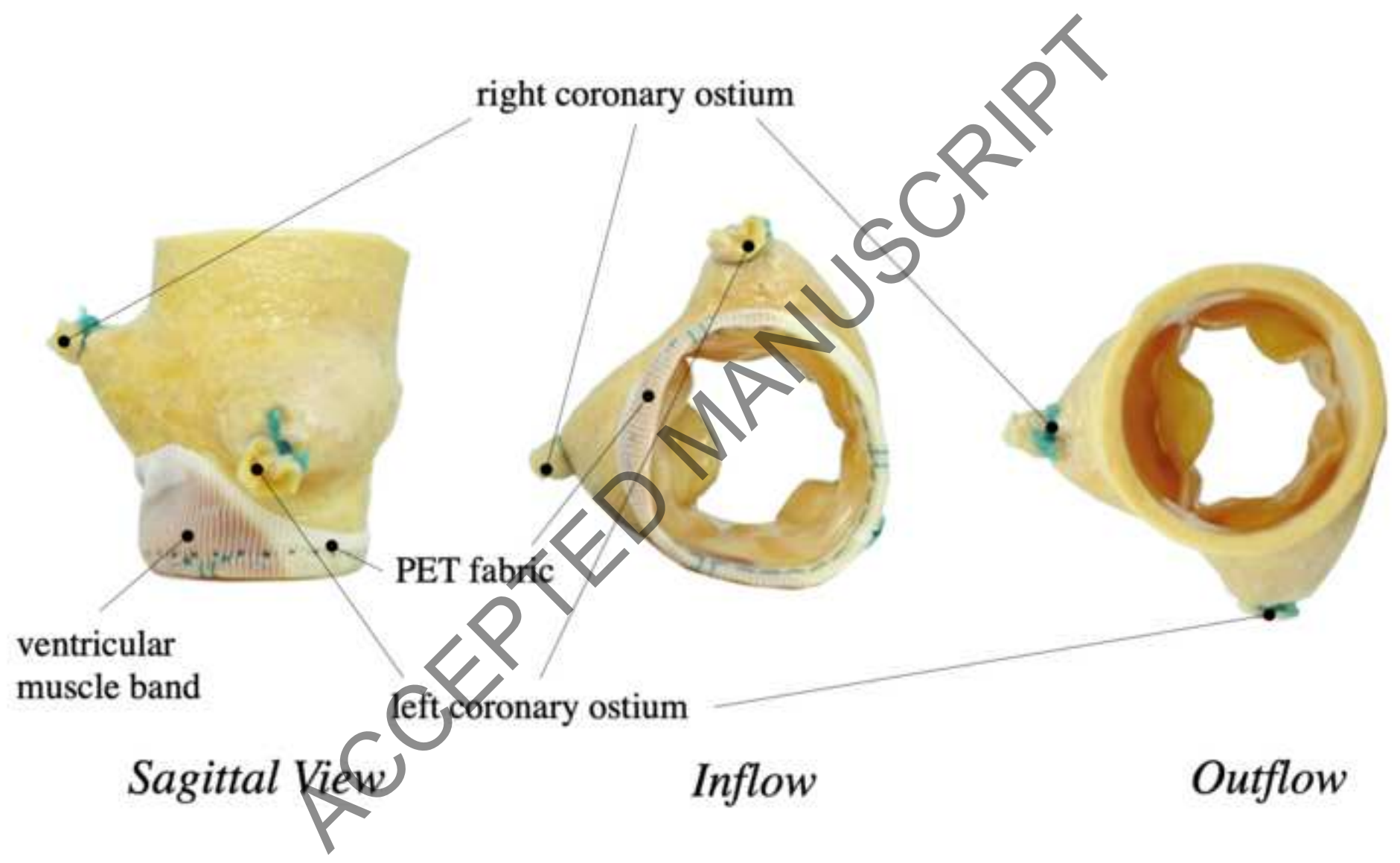
327 [2] M. J. Salameh, J. H. Black, and E. V Ratchford, "Thoracic aortic aneurysm," *Vasc. Med.*, vol. 23, no.
328 6, pp. 573–578, Dec. 2018.

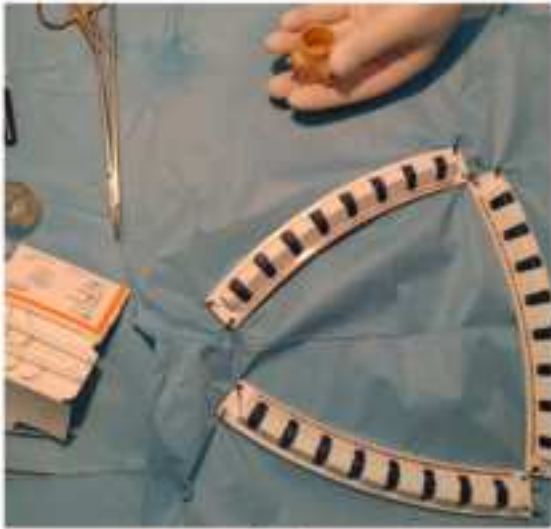
329 [3] T. E. David, "Aortic Valve Sparing in Different Aortic Valve and Aortic Root Conditions," *Journal*
330 *of the American College of Cardiology*, vol. 68, no. 6. pp. 654–664, 2016.

- 331 [4] T. E. David and C. M. Feindel, "An aortic valve-sparing operation for patients with aortic
332 incompetence and aneurysm of the ascending aorta," in *Journal of Thoracic and Cardiovascular*
333 *Surgery*, 1992, vol. 103, no. 4, pp. 617–622.
- 334 [5] M. A. I. Sarsam and M. Yacoub, "Remodeling of the aortic valve anulus," *J. Thorac. Cardiovasc.*
335 *Surg.*, vol. 105, no. 3, pp. 435–438, Mar. 1993.
- 336 [6] P. Maskell, M. Brimfield, A. Ahmed, and A. Harky, "In patients undergoing valve-sparing aortic root
337 replacement, is reimplantation superior to remodelling?," *Interactive cardiovascular and thoracic*
338 *surgery*, vol. 32, no. 3. 2021.
- 339 [7] T. Kuniyama, "Valve-sparing aortic root surgery. CON: remodeling," *Gen. Thorac. Cardiovasc. Surg.*,
340 vol. 67, no. 1, 2019.
- 341 [8] E. Beckmann *et al.*, "Comparison of Two Strategies for Aortic Valve-Sparing Root Replacement," in
342 *Annals of Thoracic Surgery*, 2020, vol. 109, no. 2, pp. 505–511.
- 343 [9] R. De Paulis, G. M. De Matteis, P. Nardi, R. Scaffa, D. F. Colella, and L. Chiarello, "A new aortic
344 Dacron conduit for surgical treatment of aortic root pathology," *Ital. Heart J.*, vol. 1, no. 7, pp. 457–
345 63, 2000.
- 346 [10] G. Pisani *et al.*, "Role of the sinuses of Valsalva on the opening of the aortic valve," *J. Thorac.*
347 *Cardiovasc. Surg.*, vol. 145, no. 4, pp. 999–1003, 2013.
- 348 [11] M. J. Paulsen *et al.*, "Comprehensive Ex Vivo Comparison of 5 Clinically Used Conduit
349 Configurations for Valve-Sparing Aortic Root Replacement Using a 3-Dimensional-Printed Heart
350 Simulator," *Circulation*, pp. 1361–1373, 2020.
- 351 [12] M. J. Paulsen *et al.*, "Modeling conduit choice for valve-sparing aortic root replacement on
352 biomechanics with a 3-dimensional-printed heart simulator," *J. Thorac. Cardiovasc. Surg.*, vol. 158,
353 no. 2, pp. 392–403, 2019.
- 354 [13] C. F. Sintek, A. D. Fletcher, and S. Khonsari, "Stentless porcine aortic root: Valve of choice for the
355 elderly patient with small aortic root?," *J. Thorac. Cardiovasc. Surg.*, vol. 109, no. 5, pp. 871–876,
356 May 1995.
- 357 [14] E. H. Kincaid and N. D. Kon, "Freestanding Root Technique for Implantation of the Stentless
358 Medtronic Freestyle Valve," *Oper. Tech. Thorac. Cardiovasc. Surg.*, vol. 11, no. 3, pp. 166–172,
359 2006.
- 360 [15] Standards Publication, "ISO 5840 - 3 Standards Publication Cardiovascular implants — Cardiac
361 valve prostheses," 2021.
- 362 [16] D. Garcia and L. Kadem, "What do you mean by aortic valve area: Geometric orifice area, effective
363 orifice area, or Gorlin area?," *J. Heart Valve Dis.*, vol. 15, no. 5, pp. 601–608, 2006.
- 364 [17] R. Toninato, J. Salmon, F. M. Susin, A. Ducci, and G. Burriesci, "Physiological vortices in the
365 sinuses of Valsalva: An in vitro approach for bio-prosthetic valves," *J. Biomech.*, vol. 49, no. 13, pp.
366 2635–2643, 2016.
- 367 [18] C. W. Akins, B. Travis, and A. P. Yoganathan, "Energy loss for evaluating heart valve performance,"

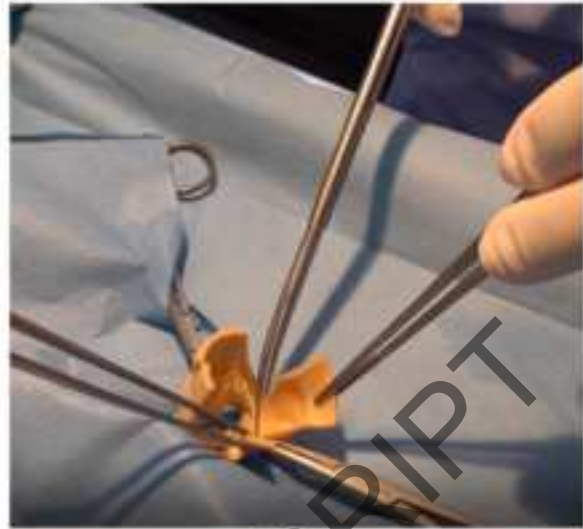
- 368 *J. Thorac. Cardiovasc. Surg.*, vol. 136, no. 4, pp. 820–833, Oct. 2008.
- 369 [19] A. M. Tango, A. Ducci, and G. Burriesci, “In silico study of the ageing effect upon aortic valves,” *J.*
370 *Fluids Struct.*, vol. 103, 2021.
- 371 [20] F. M. Susin, “Complete Unsteady One-Dimensional Model of the Net Aortic Pressure Drop,” *Open*
372 *Biomed. Eng. J.*, vol. 13, no. 1, pp. 83–93, Jun. 2019.
- 373 [21] C. C. Serdar, M. Cihan, D. Yücel, and M. A. Serdar, “Sample size, power and effect size revisited:
374 simplified and practical approaches in pre-clinical, clinical and laboratory studies,” *Biochem. medica*,
375 vol. 31, no. 1, pp. 27–53, Feb. 2021.
- 376 [22] B. J. Bellhouse and L. Talbot, “The fluid mechanics of the aortic valve,” *J. Fluid Mech.*, vol. 35, no.
377 4, pp. 721–735, Mar. 1969.
- 378 [23] B. J. BELLHOUSE, F. H. BELLHOUSE, and K. G. REID, “Fluid Mechanics of the Aortic Root with
379 Application to Coronary Flow,” *Nature*, vol. 219, no. 5158, pp. 1059–1061, Sep. 1968.
- 380 [24] A. M. Tango, J. Salmonsmith, A. Ducci, and G. Burriesci, “Validation and Extension of a Fluid–
381 Structure Interaction Model of the Healthy Aortic Valve,” *Cardiovasc. Eng. Technol.*, vol. 9, no. 4,
382 pp. 739–751, Dec. 2018.
- 383

ACCEPTED MANUSCRIPT





(a)



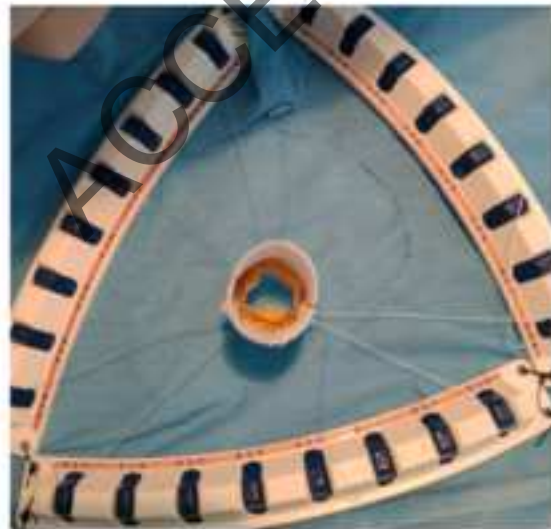
(b)



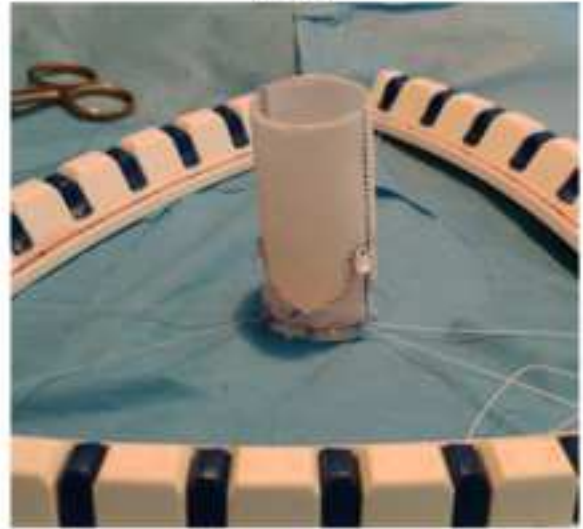
(c)



(d)

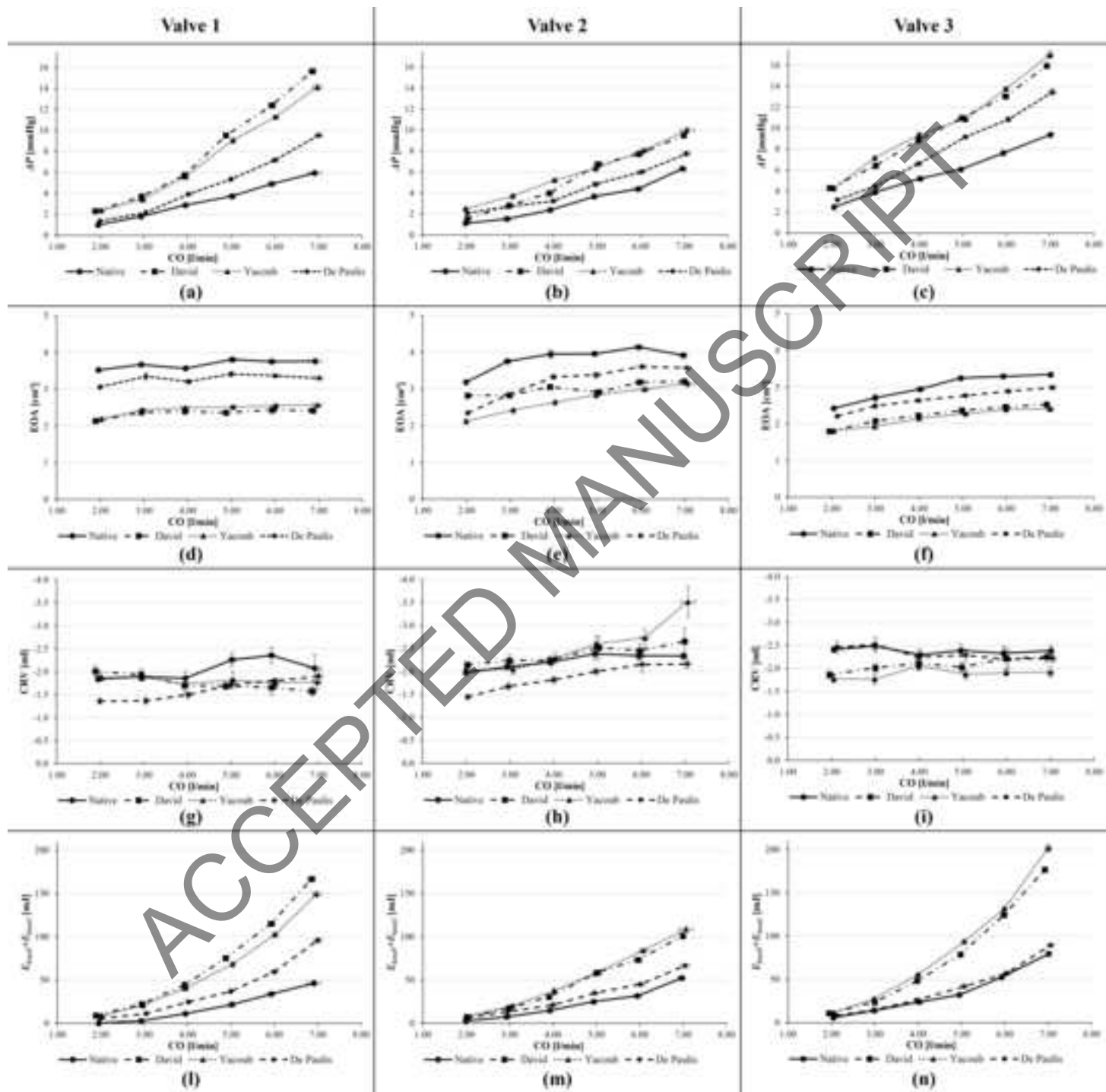


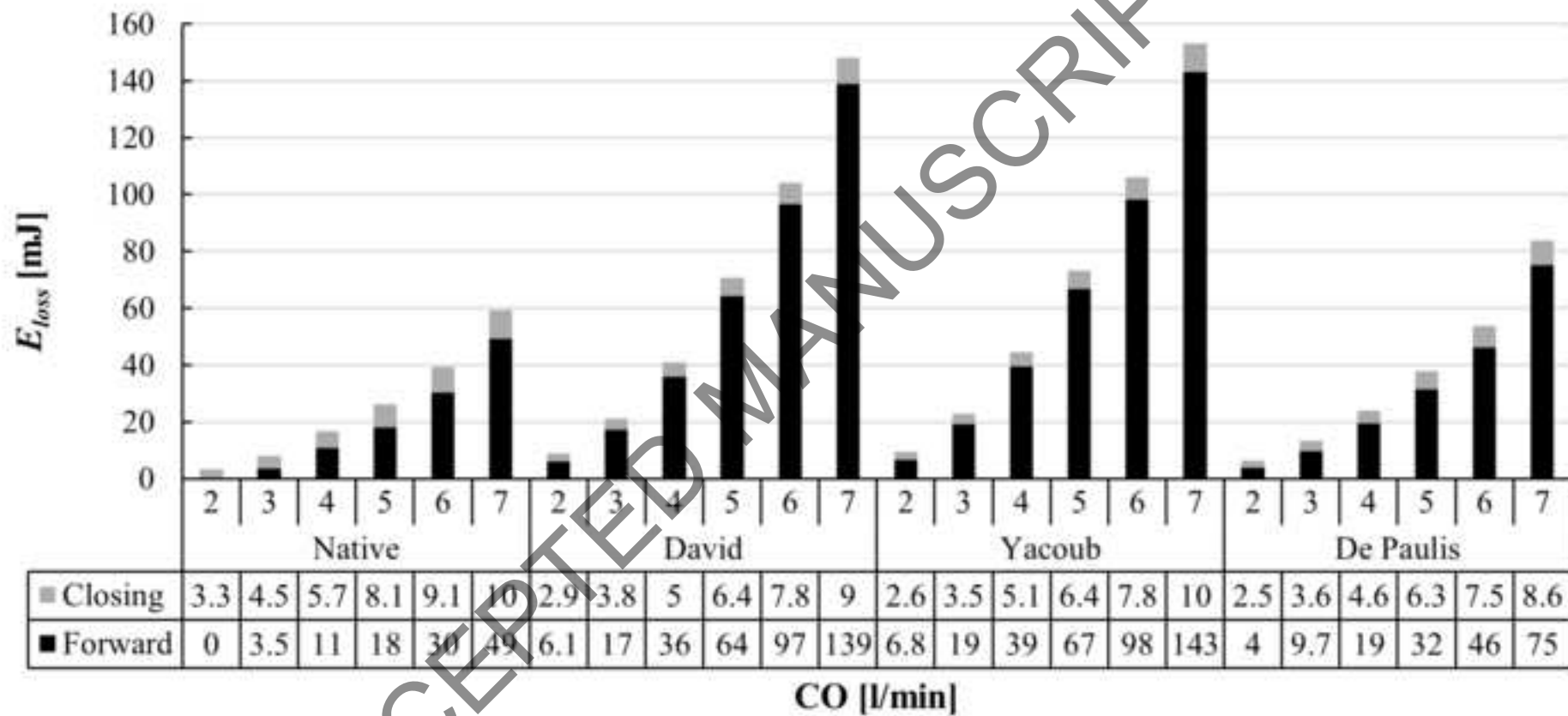
(e)



(f)









Closing ■ ■ ■ ■
Forward ■ ■ ■ ■

